PERGAMON

International Journal of Solids and Structures 39 (2002) 2939–2963

INTERNATIONAL JOURNAL OF SOLIDS and STRUCTURES

www.elsevier.com/locate/ijsolstr

# Lateral-torsional buckling of composite beams

Ákos Sapkás [a], László P. Kollár [b,*]

[a] *Research Group for Computational Structural Mechanics, Hungarian Academy of Sciences, H-1521 Budapest, Muezyetem, Hungary*
[b] *Department of Mechanics and Structures, Budapest University of Technology and Economics, Bertalan L. u.2., H-1521 Budapest, Hungary*

Received 23 May 2001; received in revised form 8 February 2002

**Abstract**

This paper presents the stability analysis of simply supported and cantilever, thin walled, open section, orthotropic composite beams subjected to concentrated end moments, concentrated forces, or uniformly distributed load. In the analysis, both the transverse shear and the restrained warping induced shear deformations are taken into account. An explicit expression is derived for the lateral-torsional buckling load of composite beams.

A simple expression is also presented, which shows the approximate reduction in the buckling load due to shear deformation. It enables us to decide whether the effect of shear deformation is negligible. 

*Keywords:* Lateral-torsional buckling; Shear deformation; Composite; Fiber reinforced plastics

## 1. Introduction

When symmetrical beams are loaded in the plane of symmetry they may deflect in the symmetry plane (Fig. 1(a)). However, at a certain level of the applied load, the beam may buckle laterally, while the cross-sections of the beam rotate simultaneously about the beam's axis (Fig. 1(b)).

This phenomenon is called lateral-torsional buckling (or lateral buckling), and the value of the load at which buckling occurs is called the buckling load or critical load.

This problem is important if the beam's transverse bending (flexural) stiffness is significantly smaller than its vertical bending stiffness.

The lateral-torsional buckling of beams was extensively treated in several books (Allen and Bulson, 1980; Galambos, 1998; Kollár, 1999; Timoshenko and Gere, 1961; Trahair, 1993) and articles (Anderson and Trahair, 1972; Clark and Hill, 1960; Helwig et al., 1997; Nethercot, 1973; Nethercot and Rockey, 1971; Roberts and Burt, 1985) in the past.

The buckling load of a simply supported beam subjected to concentrated moments ($M$) at the ends can be calculated from the following expression (Anderson and Trahair, 1972)

* Corresponding author. Tel.: +36-1-463-2393; fax: +36-1-463-1784.
*E-mail address:* lkollar@eik.bme.hu (L.P. Kollár).

0020-7683/02/$ - see front matter 
PII: S0020-7683(02)00236-6

**Nomenclature**

*List of symbols*

| | |
|---|---|
| $A$ | area of the cross-section |
| $\widehat{EA}$ | tensile stiffnesses of a composite beam |
| $\widehat{EI}_{yy}$, $\widehat{EI}_{zz}$ | bending stiffnesses of a composite beam |
| $\widehat{EI}_{\omega}$ | warping stiffness of a composite beam |
| $f$ | distance between the shear center and the location of the applied load (Fig. 2) |
| $\widehat{GI}_t$ | torsional stiffness of a composite beam |
| $h$ | plate thickness |
| $i_{\omega}$ | polar radius of gyration about the shear center (Eqs. (5) and (46)) |
| $kl$ | "effective" span |
| $l$ | span of the beam |
| $M_{\mathrm{cr}}$ | critical value of the bending moment resulting in lateral buckling |
| $M_y$, $M_z$ | bending moments in the $x$–$z$ and $x$–$y$ planes Fig. 6 |
| $M_{\omega}$ | bimoment |
| $\widehat{N}^{\mathrm{B}}_{\mathrm{cr}z}$ | Euler buckling load in the $x$–$y$ plane (no shear deformation) |
| $\widehat{N}^{\mathrm{B}}_{\mathrm{cr}\psi}$ | torsional buckling load referred to the shear center (no shear deformation) |
| $\widehat{N}^{\mathrm{B}}_{\mathrm{cr}\omega}$ | torsional buckling load when $\widehat{EI}_{\omega} \gg \widehat{GI}_t$ (no shear deformation) |
| $\widehat{N}^{\mathrm{BS}}_{\mathrm{cr}z}$ | Euler buckling load in the $x$–$y$ plane (with shear deformation) |
| $\widehat{N}^{\mathrm{BS}}_{\mathrm{cr}\psi}$ | torsional buckling load referred to the shear center (with shear deformation) |
| $\widehat{N}^{\mathrm{BS}}_{\mathrm{cr}\omega}$ | torsional buckling load when $\widehat{EI}_{\omega} \gg \widehat{GI}_t$ (with shear deformation) |
| $p_y$, $p_z$ | transverse loads (per unit length) acting on a beam (Fig. 6) |
| $P_{\mathrm{cr}}$ | critical value of the concentrated force resulting in lateral buckling |
| $q_{\mathrm{cr}}$ | critical value of the uniformly distributed load resulting in lateral buckling |
| $\widehat{S}_{yy}$, $\widehat{S}_{zz}$, $\widehat{S}_{y\omega}$, $\widehat{S}_{\omega\omega}$ | shear stiffnesses of a beam |
| $t$ | torque load (per unit length) acting on a beam (Fig. 6) |
| $T$ | torque (Fig. 6) |
| $T_{\mathrm{sv}}$ | Saint Venant torque |
| $T_{\omega}$ | restrained warping induced torque |
| $U$ | strain energy |
| $u$, $w$ | displacement in the $y$ and $z$ directions |
| $V_y$, $V_z$ | shear forces (Fig. 6) |
| $W$ | work done by the external load |
| $z_{\mathrm{sc}}$ | coordinates of the shear center (Fig. 2) |
| $\alpha$ | reduction in the buckling load due to the shear deformation |
| $\beta_1$ | cross-sectional property (Eq. (21)) |
| $\gamma_y$, $\gamma_z$ | shear strains in the $x$–$y$ and the $x$–$z$ planes |
| $\vartheta$ | twist per unit length |
| $\vartheta_{\mathrm{B}}$ | twist per unit length, when there is no shear deformation |
| $\vartheta_{\mathrm{S}}$ | twist per unit length due to the shear deformation of the wall |
| $\kappa_y$, $\kappa_z$ | derivatives of $\chi_y$, and $\chi_z$ (Eq. (12)) |
| $\chi_y$, $\chi_z$ | rotations of the cross-section about the $z$- and $y$-axes |
| $\psi$ | rotation of the cross-section about the $x$-axis (angle of twist) |
| $\Pi$ | potential energy of the beam |

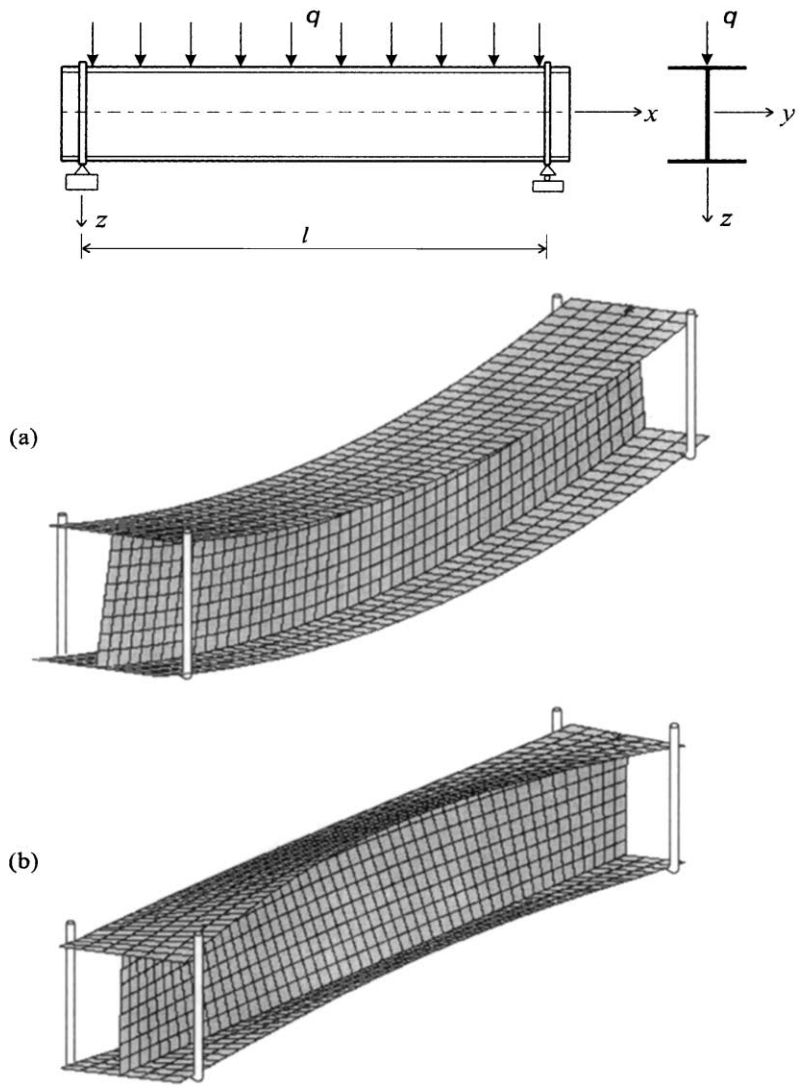


Fig. 1. In plane (a) and lateral-torsional (b) deformation of a symmetrical beam loaded in the symmetry plane.

$$M_{\mathrm{cr}}^2 - \widehat{N}_{\mathrm{crz}}^{\mathrm{B}} \beta_1 M_{\mathrm{cr}} - \widehat{N}_{\mathrm{crz}}^{\mathrm{B}} \widehat{N}_{\mathrm{cr}\psi}^{\mathrm{B}} i_\omega^2 = 0, \tag{1}$$

where $\beta_1$ is a cross-sectional property (given in Section 4.1), and

$$\widehat{N}_{\mathrm{crz}}^{\mathrm{B}} = \frac{\pi^2}{l^2} EI_{zz} \tag{2}$$

is the Euler buckling load of a simply supported slender beam subjected to concentrated axial forces at the ends if the beam buckles in $x$–$y$ plane, $l$ is the length of the beam, $EI_{zz}$ is the bending stiffness about the vertical ($z$) axis (Fig. 1), while

$$\widehat{N}^{\mathrm{B}}_{\mathrm{cr}\psi} = \widehat{N}^{\mathrm{B}}_{\mathrm{cr}\omega} + \frac{1}{i_\omega^2} GI_t \tag{3}$$

is the buckling load of the same beam if it buckles torsionally about the shear center. Here

$$\widehat{N}^{\mathrm{B}}_{\mathrm{cr}\omega} = \frac{1}{i_\omega^2}\frac{\pi^2}{l^2} EI_\omega \tag{4}$$

is the torsional buckling load when $EI_\omega \gg GI_t$, where $GI_t$ and $EI_\omega$ are the torsional and the warping stiffnesses, respectively. $i_\omega$ is the polar radius of gyration of the cross-section about the shear center

$$i_\omega^2 = z_{\mathrm{sc}}^2 + \frac{I_{yy} + I_{zz}}{A}, \tag{5}$$

where $z_{\mathrm{sc}}$ is the distance between the shear center (SC) and the centroid (C) (Fig. 2). $I_{yy}$ and $I_{zz}$ are the second moments of area about axes $y$ and $z$, respectively, and $A$ is the area of the cross-section.

Eq. (1) yields

$$M_{\mathrm{cr}} = \widehat{N}^{\mathrm{B}}_{\mathrm{cr}z}\left(\frac{\beta_1}{2} + \sqrt{\left(\frac{\beta_1}{2}\right)^2 + \frac{\widehat{N}^{\mathrm{B}}_{\mathrm{cr}\psi} i_\omega^2}{\widehat{N}^{\mathrm{B}}_{\mathrm{cr}z}}}\right). \tag{6}$$

The buckling load of a simply supported beam subjected to uniformly distributed load ($q$) is given by the root of the following equation (Kollár, 1999):

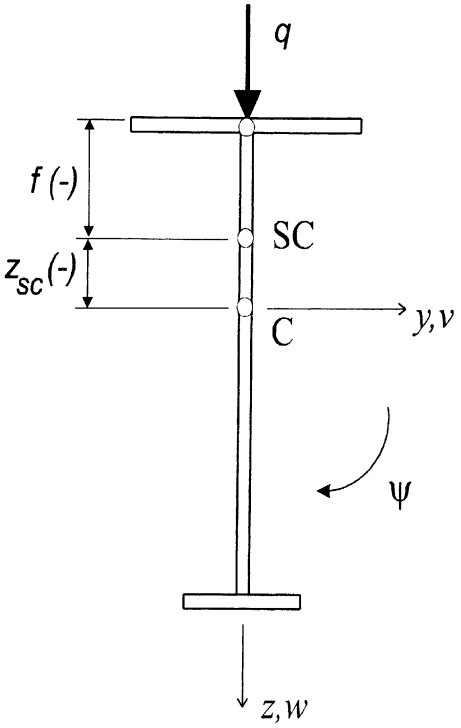


Fig. 2. Location of the shear center and the applied load.

$$\underbrace{\left(\frac{\pi^2+3}{12\pi^2}\right)^2}_{0.01181} l^4 q_{\mathrm{cr}}^2 - \left(\underbrace{\frac{\pi^2-3}{12\pi^2}}_{0.05800}\beta_1 + \underbrace{\frac{1}{\pi^2}}_{0.10132} f\right) l^2 \widehat{N}^{\mathrm{B}}_{\mathrm{crz}} q_{\mathrm{cr}} - \widehat{N}^{\mathrm{B}}_{\mathrm{crz}} \widehat{N}^{\mathrm{B}}_{\mathrm{cr}\psi} i_\omega^2 = 0, \tag{7}$$

which yields

$$M_{\mathrm{cr}} = \frac{q_{\mathrm{cr}} l^2}{8} = 1.15 \widehat{N}^{\mathrm{B}}_{\mathrm{crz}} \left(0.466 f + 0.267\beta_1 + \sqrt{(0.466 f + 0.267\beta_1)^2 + \frac{\widehat{N}^{\mathrm{B}}_{\mathrm{cr}\psi} i_\omega^2}{\widehat{N}^{\mathrm{B}}_{\mathrm{crz}}}}\right). \tag{8}$$

In these equations $f$ is the distance between the shear center and the location of the applied load (Fig. 2) and $l$ is the length of the beam.

Clark and Hill (1960) presented a formula (see also Allen and Bulson, 1980) for the buckling load of simply supported and cantilever beams in the form

$$M_{\mathrm{cr}} = C_1 \frac{\pi^2}{(kl)^2} \widehat{EI}_{zz} \left(C_2 f + C_3\beta_1 + \sqrt{(C_2 f + C_3\beta_1)^2 + \frac{\widehat{EI}_\omega}{\widehat{EI}_{zz}}\left(1 + \frac{\widehat{GI}_t}{\widehat{EI}_\omega}\frac{(kl)^2}{\pi^2}\right)}\right), \tag{9}$$

where $C_1$, $C_2$, $C_3$ are constants and $M_{\mathrm{cr}}$ is the critical value of the maximum bending moment, which is related to the loads (see Table 1). $k = 1$ for a cantilever beam otherwise it depends on the end conditions for a simply supported beam. When the rotation of the end cross-sections are not restrained about the $z$-axis $k = 1$, when these rotations and warping are restrained $k = 0.5$. (The constants $C_1$, $C_2$, $C_3$ in Table 1 were taken from Clark and Hill (1960) for all the cases except for case *d*. For this case the constants were determined in Section 5.4.)

Note that the constants for the simply supported beam agree within 5% of those given in Eqs. (6) and (8), which is negligible for practical purposes. We also note that Eq. (9) gives the accurate value of the buckling load for concentrated moments.

Care should be taken when Eq. (9) is applied to short cantilever beams subjected to loads *above* or *below* the shear center. By numerical comparison we obtained that for short beams Eq. (9) gives reasonable value for the critical load only if the beam is subjected at the shear center (see Section 7).

When pultruted composite beams are made of unidirectional carbon fibers the longitudinal Young modulus may be 20–30 times higher than the shear modulus, which means that the effect of shear deformation is higher by an order of magnitude than that of isotropic beams. Pultruted beams are often made of

Table 1
Parameters in Eq. (9)

| | $C_1$ | $C_2$ | $C_3$ |
|---|---|---|---|
| *Simply supported beam ($k=1$)* | | | |
| (a) End moments | 1 | 0 | 0.5 |
| (b) Uniformly distributed load ($M_{\mathrm{cr}} = q_{\mathrm{cr}} l^2/8$) | 1.13 | 0.45 | 0.267 |
| (c) Concentrated force ($M_{\mathrm{cr}} = P_{\mathrm{cr}} l/4$) | 1.35 | 0.55 | 0.212 |
| (d) Two concentrated forces ($M_{\mathrm{cr}} = P_{\mathrm{cr}} l/3$) | 1.12 | 0.51 | 0.245 |
| *Simply supported beam (the rotations (about the z-axis) and the warping of the end cross-sections are restrained, $k=0.5$)* | | | |
| (a) Concentrated force ($M_{\mathrm{cr}} = P_{\mathrm{cr}} l/4$) | 1.07 | 0.42 | n.a |
| *Cantilever beam ($k=1$)* | | | |
| (a) Distributed load ($M_{\mathrm{cr}} = q_{\mathrm{cr}} l^2/2$) | 2.05 | n.a | n.a |
| (b) Concentrated force ($M_{\mathrm{cr}} = P_{\mathrm{cr}} l$) | 1.28 | n.a | n.a |

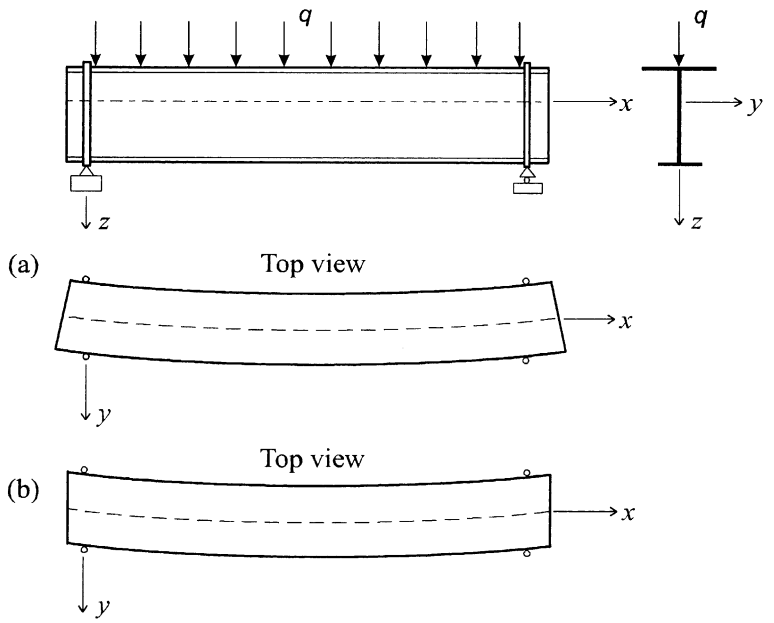


Fig. 3. Horizontal displacement of a beam when the shear deformation is neglected (a), and when only the shear deformation is taken into account (b).

glass fibers with about 50% of unidirectional fibers and 50% of continuous mat. For such beams the ratio of the Young modulus and the shear modulus is in the range of 5–10. The horizontal displacements of the beam is illustrated in Fig. 3. When there is no shear deformation the beam deforms as shown in Fig. 3(a), while when there is only shear deformation (no bending deformation) the deformed beam is illustrated in Fig. 3(b).

Several authors investigated the lateral-torsional buckling of pultruted composite beams (Brooks and Turvey, 1995; Davalos and Qiao, 1997; Davalos et al., 1997; Johnson and Shield, 1998; Lin et al., 1996; Mottram, 1992; Pandey et al., 1995; Sherbourne and Kabir, 1995; Turvey, 1996; Zureick et al., 1995) and although most of the authors mention the effect of the shear deformation only Sherbourne and Kabir (1995) considered it in their analytical result. In their article they took the transverse shear deformation into account but they neglected the shear deformation in torsion. They considered simply supported beams with doubly symmetric cross-section subjected to loads acting at the shear center.

In this paper we wish to determine the lateral-torsional buckling load of composite beams taking both the lateral and torsional shear deformation into account. (The cross-section of the beam may be mono-symmetrical and the beam may be loaded above or below the shear center.)

## 2. Problem statement

We consider symmetrical cross-section prismatic beams loaded in the plane of symmetry. The beam is either simply supported at both ends (Fig. 4) or one end is built in and the other is free (cantilever, Fig. 5). A simple support restrains the displacements and the rotation about the beam's $x$-axis, but allows the rotation about the $y$- and $z$-axes, and the warping of the cross-section.

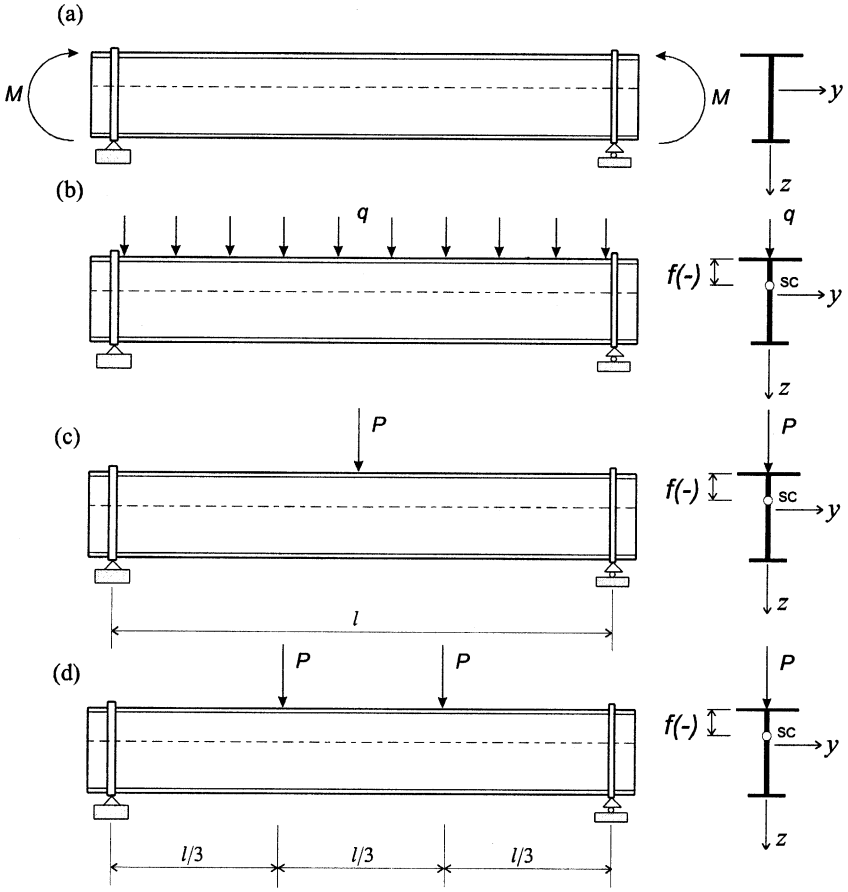


Fig. 4. Simply supported beams.

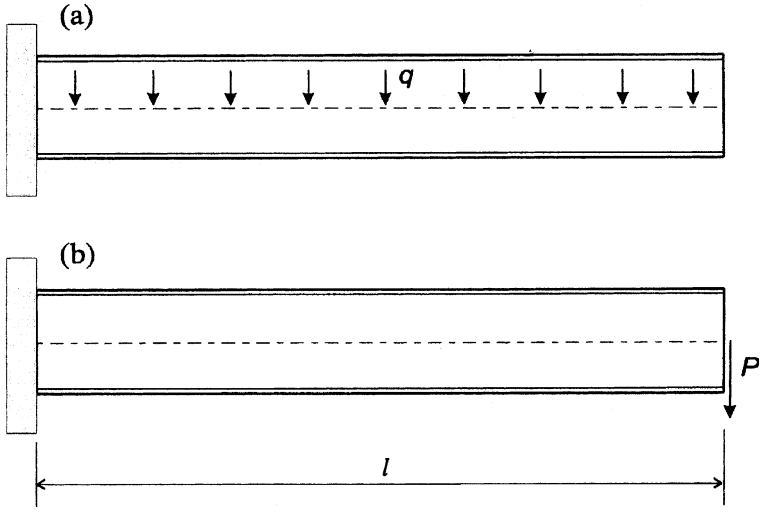


Fig. 5. Cantilever beams.

The simply supported beam may be loaded by concentrated moments at the ends (Fig. 4(a)), by a uniformly distributed load acting at a distance $f$ from the shear center of the beam (Fig. 4(b)), by a concentrated load at the midspan (Fig. 4(c)) or by two concentrated forces at the thirds of the span (Fig. 4(d)).

The cantilever beam may be loaded at the shear center by a uniformly distributed load (Fig. 5(a)) or by a concentrated force (Fig. 5(b)). The loads are acting at the shear center.

We determine the critical load of the beam subjected to the above mentioned loads.

## 3. Approach

The critical load of a beam can be determined analytically, numerically, or by experiments. Here, our main interest is to derive explicit expressions for the buckling loads. However, we will use a commercially available FE code (ANSYS, 1997) to verify our results numerically, and we will also compare our results to experimental data from the literature.

It is assumed that the material behaves in a linearly elastic manner and the deformations are small. We are interested only in the bifurcation load, the deformations prior to buckling are not considered.

Under the applied loads the beam may buckle globally or its walls may buckle locally (plate buckling). Here local buckling of the members (such as web or flanges) are not considered.

When modelling the beam "first order shear theory" is applied. Beams may undergo transverse and torsional shear deformation which must be taken into account. Wu and Sun (1992) suggested a model to account for the torsional shear deformation, which was simplified in Kollár (2001a). This latter model is adopted here.

## 4. Governing equations

The governing equations of the beam theory are summarized below. The equilibrium equations, the strain–stress relationship and the constitutive equations are as follows (Kollár, 2001a):

*Equilibrium equations*:

$$\frac{\mathrm{d}M_z}{\mathrm{d}x} = V_y, \quad \frac{\mathrm{d}M_y}{\mathrm{d}x} = V_z, \quad \frac{\mathrm{d}M_\omega}{\mathrm{d}x} = T_\omega, \quad \frac{\mathrm{d}V_y}{\mathrm{d}x} = -p_y, \quad \frac{\mathrm{d}V_z}{\mathrm{d}x} = -p_z, \quad \frac{\mathrm{d}T_{\mathrm{sv}}}{\mathrm{d}x} + \frac{\mathrm{d}T_\omega}{\mathrm{d}x} = -t, \tag{10}$$

where $M_z$, $V_y$, $p_y$ and $M_y$, $V_z$, $p_z$ are the bending moment, the shear force and the external load in the $y$–$x$ and $z$–$x$ planes, respectively. $M_\omega$ is the bimoment, and $t$ is the distributed torque load (Fig. 6). $T_{\mathrm{sv}}$ and $T_\omega$ are the Saint-Venant torque and the restrained warping induced torque respectively and the total torque ($T$) is

$$T = T_{\mathrm{sv}} + T_\omega. \tag{11}$$

*Strain–displacement relationships*:

$$\kappa_z = -\frac{\mathrm{d}\chi_y}{\mathrm{d}x}, \quad \kappa_y = -\frac{\mathrm{d}\chi_z}{\mathrm{d}x}, \quad \vartheta = \frac{\mathrm{d}\psi}{\mathrm{d}x}, \quad \Gamma = -\frac{\mathrm{d}\vartheta_{\mathrm{B}}}{\mathrm{d}x}, \quad \vartheta_{\mathrm{S}} = \frac{\mathrm{d}\psi}{\mathrm{d}x} - \vartheta_{\mathrm{B}}, \quad \gamma_y = \frac{\mathrm{d}v}{\mathrm{d}x} - \chi_y, \quad \gamma_z = \frac{\mathrm{d}w}{\mathrm{d}x} - \chi_z, \tag{12}$$

where $v$ and $w$ are the displacements in the $y$–$x$ and $z$–$x$ planes, $\psi$ is the rotation of the cross-section about the $x$-axis (angle of twist). $\chi_y$ and $\chi_z$ are the rotations of the cross-section about the $z$- and $y$-axes; while $\vartheta_{\mathrm{B}}$ is the twist per unit length, when there is no shear deformation present in the beam. $\gamma_y$ and $\gamma_z$ are the shear strains in the $x$–$y$ and the $x$–$z$ planes, while $\vartheta_{\mathrm{S}}$ is the twist per unit length due to the shear deformation of

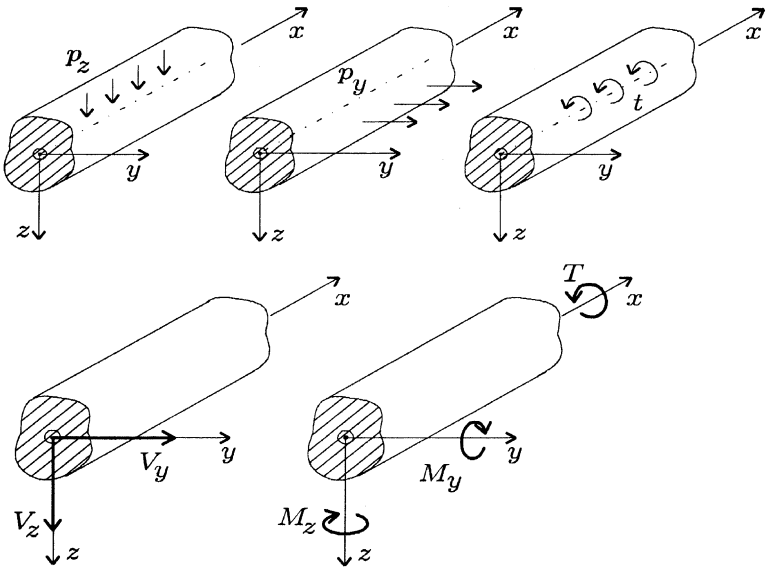


Fig. 6. Transverse and torque loads acting on the beam (top), internal moments and shear forces (bottom).

the wall (see also Roberts and Al-Ubaidi, 2001). We note that in the presented theory the first derivative of the displacements are

$$\frac{\mathrm{d}v}{\mathrm{d}x} = \chi_y + \gamma_y, \quad \frac{\mathrm{d}w}{\mathrm{d}x} = \chi_z + \gamma_z, \quad \frac{\mathrm{d}\psi}{\mathrm{d}x} = \vartheta_{\mathrm{B}} + \vartheta_{\mathrm{S}}, \tag{13}$$

while if there is no shear deformation (e.g. in Vlasov's beam theory), $\gamma_y = \gamma_z = \vartheta_{\mathrm{S}} = 0$, the derivatives are:

$$\frac{\mathrm{d}v}{\mathrm{d}x} = \chi_y, \quad \frac{\mathrm{d}w}{\mathrm{d}x} = \chi_z, \quad \frac{\mathrm{d}\psi}{\mathrm{d}x} = \vartheta_{\mathrm{B}}. \tag{14}$$

*Constitutive equations*: Considering a cross-section which is symmetrical with respect to the $z$-axis, the constitutive equations are (Kollár, 2001a):

$$\begin{Bmatrix} M_z \\ M_y \\ M_\omega \end{Bmatrix} = \begin{bmatrix} \widehat{EI}_{zz} & 0 & 0 \\ 0 & \widehat{EI}_{yy} & 0 \\ 0 & 0 & \widehat{EI}_{\omega} \end{bmatrix} \begin{Bmatrix} \kappa_z \\ \kappa_y \\ \Gamma \end{Bmatrix}, \tag{15}$$

$$\begin{Bmatrix} V_y \\ V_z \\ T_\omega \end{Bmatrix} = \begin{bmatrix} \widehat{S}_{yy} & 0 & \widehat{S}_{y\omega} \\ 0 & \widehat{S}_{zz} & 0 \\ \widehat{S}_{y\omega} & 0 & \widehat{S}_{\omega\omega} \end{bmatrix} \begin{Bmatrix} \gamma_y \\ \gamma_z \\ \vartheta_{\mathrm{S}} \end{Bmatrix}, \tag{16}$$

$$T_{\mathrm{sv}} = \widehat{GI}_t \vartheta, \tag{17}$$

where $\widehat{EI}_{zz}$, $\widehat{EI}_{yy}$, $\widehat{EI}_{\omega}$, and $\widehat{GI}_t$ are the bending, warping and torsional stiffnesses of a composite beam, respectively. (For isotropic beams the same expressions are applicable without the "hats".)

The calculation of the stiffnesses ($\widehat{EI}_{zz}$, $\widehat{EI}_{yy}$, $\widehat{EI}_{\omega}$, $\widehat{GI}_t$, $\widehat{S}_{yy}$, $\widehat{S}_{zz}$, $\widehat{S}_{\omega\omega}$, $\widehat{S}_{y\omega}$) are given in Kollár (2001b), and the formulas for a monosymmetric I-beam are summarized in Appendix A.

### 4.1. Governing equations for lateral-torsional buckling

The governing equations for lateral-torsional buckling of beams without shear deformation are given in Kollár (1999). The equilibrium equations, regardless of the presence of the shear deformation, are

$$\frac{\mathrm{d}M_z}{\mathrm{d}x} = V_y, \qquad \frac{\mathrm{d}M_\omega}{\mathrm{d}x} = T_\omega, \tag{18}$$

$$\frac{\mathrm{d}V_y}{\mathrm{d}x} = -p_y, \qquad \frac{\mathrm{d}T_{\mathrm{sv}}}{\mathrm{d}x} + \frac{\mathrm{d}T_\omega}{\mathrm{d}x} = -t, \tag{19}$$

where

$$p_y = -\frac{\mathrm{d}^2(M_y\psi)}{\mathrm{d}x^2}, \qquad t = -M_y\frac{\mathrm{d}^2 v}{\mathrm{d}x^2} f \frac{\mathrm{d}^2 M_y}{\mathrm{d}x^2}\psi + \beta_1\frac{\mathrm{d}}{\mathrm{d}x}\left(M_y\frac{\mathrm{d}\psi}{\mathrm{d}x}\right). \tag{20}$$

$M_y$ is the horizontal bending moment of the beam in the $z$–$x$ plane which can be calculated from the vertical loads, and $f$ is the distance of this load from the shear center.

$\beta_1$ is a cross-sectional property defined for an isotropic cross-section beam as (see Kollár, 1999)

$$\beta_1 = J_1 + J_2 - 2z_{\mathrm{sc}}. \tag{21}$$

For a beam made of isotropic material $J_1$ and $J_2$ are

$$J_1 = \frac{1}{I_{yy}}\int_{(A)} z^3\,\mathrm{d}A, \qquad J_2 = \frac{1}{I_{yy}}\int_{(A)} zy^2\,\mathrm{d}A. \tag{22}$$

For a thin walled, open section, isotropic beam $J_1$ and $J_2$ may be written as

$$J_1 = \frac{1}{EI_{yy}}\int_{(S)} (Eh)z^3\,\mathrm{d}\eta, \qquad J_2 = \frac{1}{EI_{yy}}\int_{(S)} (Eh)zy^2\,\mathrm{d}\eta, \tag{23}$$

where $h$ is the thickness of the wall and $\eta$ is the coordinate along the perimeter. For an orthotropic symmetrical lay-up beam, $Eh$ is replaced by $1/a_{11}$ and $EI_{yy}$ is replaced by $\widehat{EI}_{yy}$. This gives

$$J_1 = \frac{1}{\widehat{EI}_{yy}}\int_{(S)} \frac{1}{a_{11}}z^3\,\mathrm{d}\eta, \qquad J_2 = \frac{1}{\widehat{EI}_{yy}}\int_{(S)} \frac{1}{a_{11}}zy^2\,\mathrm{d}\eta. \tag{24}$$

For an orthotropic I-beam these integrals result in

$$\begin{aligned} J_1 &= \frac{1}{\widehat{EI}_{yy}}\left(-\frac{1}{(a_{11})_{f_1}}b_{f_1}(d-z_{\mathrm{c}})^3 + \frac{1}{(a_{11})_{f_2}}b_{f_2}z_{\mathrm{c}}^3 - \frac{1}{(a_{11})_\omega}\frac{b_{\omega1}^4 - b_{\omega2}^4}{4}\right),\\ J_2 &= \frac{1}{\widehat{EI}_{yy}}\left(-\frac{1}{(a_{11})_{f_1}}\frac{b_{f_1}^3}{12}(d-z_{\mathrm{c}}) + \frac{1}{(a_{11})_{f_2}}\frac{b_{f_2}^3}{12}z_{\mathrm{c}}\right). \end{aligned} \tag{25}$$

The symbols are defined in Appendix A.

We note that for a doubly symmetric cross-section beam $\beta_1 = J_1 = J_2 = 0$.

In the above equilibrium equations the bending moment $M_y$ is known, and the shear force $V_z$ does not appear. The relevant part of the strain–displacement equations (Eq. (12)) is

$$\kappa_z = -\frac{d\chi_y}{dx}, \qquad \vartheta = \frac{d\psi}{dx}, \tag{26}$$

$$\Gamma = -\frac{d\vartheta_B}{dx}, \qquad \vartheta_S = \frac{d\psi}{dx} - \vartheta_B, \tag{27}$$

$$\gamma_y = \frac{dv}{dx} - \chi_y, \tag{28}$$

while the relevant part of the strain–stress relationship (Eqs. (15)–(17)) is

$$\begin{aligned}
&\left\{ \begin{array}{c} M_z \\ M_\omega \end{array} \right\} = \left[ \begin{array}{cc} \widehat{EI}_{zz} & 0 \\ 0 & \widehat{EI}_\omega \end{array} \right] \left\{ \begin{array}{c} \kappa_z \\ \Gamma \end{array} \right\}, \\
&\left\{ \begin{array}{c} V_y \\ T_\omega \end{array} \right\} = \left[ \begin{array}{cc} \widehat{S}_{yy} & \widehat{S}_{y\omega} \\ \widehat{S}_{y\omega} & \widehat{S}_{\omega\omega} \end{array} \right] \left\{ \begin{array}{c} \gamma_y \\ \vartheta_S \end{array} \right\}, \\
&T_{sv} = \widehat{GI}_t \vartheta.
\end{aligned} \tag{29}$$

## 5. Simply supported beams

In this section simply supported beams are considered (Fig. 4).

### 5.1. End moments

When the beam is subjected to concentrated bending moments at the ends (Fig. 4(a)) Eq. (20) simplifies to

$$p_y = -M_y \frac{\mathrm{d}^2\psi}{\mathrm{d}x}, \qquad t = -M_y \frac{\mathrm{d}^2 v}{\mathrm{d}x} + \beta_1 M_y \frac{\mathrm{d}^2\psi}{\mathrm{d}x}. \tag{30}$$

When the beam is *simply supported* the displacements in the $y$ direction and the rotation about the $x$-axis are zero

$$v = 0, \qquad \psi = 0 \quad \text{at } x = 0, l. \tag{31}$$

The end cross-sections may rotate about the $z$-axis and is free to warp, hence

$$M_z = 0, \qquad M_\omega = 0 \quad \text{at } x = 0, l. \tag{32}$$

The following displacement functions satisfy the boundary conditions:

$$\begin{array}{ll} v = v_0 \sin\frac{i\pi x}{l}, & \chi_y = \chi_0 \cos\frac{i\pi x}{l}, \\ \psi = \psi_0 \sin\frac{i\pi x}{l}, & \vartheta_B = \vartheta_0^B \cos\frac{i\pi x}{l}. \end{array} \quad i = 1, 2, \ldots \tag{33}$$

The deformation of the beam for $i = 1$ is illustrated in Fig. 1(b). At the supports the beam rotates about the $z$- and $y$-axes and the cross-section warps, however the rotation of the cross-section about the $z$-axis is zero. (We note that these displacement functions satisfy the governing equations.)

By substituting Eq. (33) into Eqs. (26)–(28) and Eq. (30), then $\kappa_z$, $\Gamma$ and $\gamma_y$, $\vartheta_S$ and $\vartheta$ into Eq. (29) and the obtained expressions for $M_z$, $M_\omega$ and $V_y$, $T_\omega$, $T_{sv}$ and $p_y$, $t$ into the equilibrium equations (Eqs. (18) and (19)), after algebraic manipulation Eq. (18) gives

$$\left( \left( \frac{i^2\pi^2}{l^2} [\widehat{EI}] + [\widehat{S}] \right) \left\{ \begin{array}{c} \chi_0 \\ \vartheta_0^B \end{array} \right\} - \frac{i\pi}{l} [\widehat{S}] \left\{ \begin{array}{c} v_0 \\ \psi_0 \end{array} \right\} \right) \cos\frac{i\pi x}{l} = 0, \tag{34}$$

and Eq. (19) results in

$$\left(\left(\frac{i^2\pi^2}{l^2}[\widehat{S}]+\frac{i^2\pi^2}{l^2}\begin{bmatrix}0 & 0\\ 0 & \widehat{GI}_t\end{bmatrix}+\frac{i^2\pi^2}{l^2}M_{\mathrm{cr}}\begin{bmatrix}0 & -1\\ -1 & \beta_1\end{bmatrix}\right)\begin{Bmatrix}v_0\\ \psi_0\end{Bmatrix}-\frac{i\pi}{l}[\widehat{S}]\begin{Bmatrix}\chi_0\\ \vartheta_0^{\mathrm{B}}\end{Bmatrix}\right)\sin\frac{i\pi x}{l}=0, \tag{35}$$

where

$$[\widehat{EI}]=\begin{bmatrix}\widehat{EI}_{zz} & 0\\ 0 & \widehat{EI}_{\omega}\end{bmatrix}, \tag{36}$$

$$[\widehat{S}]=\begin{bmatrix}\widehat{S}_{yy} & \widehat{S}_{y\omega}\\ \widehat{S}_{y\omega} & \widehat{S}_{\omega\omega}\end{bmatrix}. \tag{37}$$

By eliminating $\chi_0$ and $\vartheta_0^{\mathrm{B}}$ from Eqs. (34) and (35) we obtain

$$\left([\widehat{S}]-[\widehat{S}]\left(\frac{i^2\pi^2}{l^2}[\widehat{EI}]+[\widehat{S}]\right)^{-1}[\widehat{S}]+\begin{bmatrix}0 & 0\\ 0 & \widehat{GI}_t\end{bmatrix}+M_{\mathrm{cr}}\begin{bmatrix}0 & -1\\ -1 & \beta_1\end{bmatrix}\right)\begin{Bmatrix}v_0\\ \psi_0\end{Bmatrix}=0. \tag{38}$$

The lowest buckling load is obtained if $i=1$. With this substitution the condition of the nontrivial solution is

$$\left|[Q]+M_{\mathrm{cr}}\begin{bmatrix}0 & -1\\ -1 & \beta_1\end{bmatrix}\right|=0, \tag{39}$$

where

$$[Q]=\left(\frac{1}{\frac{\pi^2}{l^2}}[\widehat{EI}]^{-1}+[\widehat{S}]^{-1}\right)^{-1}+\begin{bmatrix}0 & 0\\ 0 & \widehat{GI}_t\end{bmatrix}. \tag{40}$$

Eq. (39) results in a second order equation to determine the critical bending moment, $M_{\mathrm{cr}}$. (Since the assumed displacement functions Eq. (33) satisfy both the boundary conditions and the governing equations the derived expression for $M_{\mathrm{cr}}$ results in the exact buckling moment.)

*Approximate solution*: The solution simplifies when the cross-section is doubly symmetric, and hence, $\widehat{S}_{y\omega}=0$. This condition can be taken as an approximation for cross-sections which are symmetrical only about the $z$-axis:

$$\widehat{S}_{y\omega}\approx 0. \tag{41}$$

In this case matrix $[Q]$ becomes

$$[Q]=\begin{bmatrix}\widehat{N}_{\mathrm{cr}z}^{\mathrm{BS}} & 0\\ 0 & i_{\omega}^2\widehat{N}_{\mathrm{cr}\psi}^{\mathrm{BS}}\end{bmatrix}, \tag{42}$$

where

$$\widehat{N}_{\mathrm{cr}z}^{\mathrm{BS}}=\left(\frac{1}{\widehat{N}_{\mathrm{cr}z}^{\mathrm{B}}}+\frac{1}{\widehat{S}_{yy}}\right)^{-1}, \tag{43}$$

$$\widehat{N}_{\mathrm{cr}\psi}^{\mathrm{BS}}=\widehat{N}_{\mathrm{cr}\omega}^{\mathrm{BS}}+\frac{1}{i_{\omega}^2}\widehat{GI}_t. \tag{44}$$

Eq. (43) was first derived by Engesser (1889). Here

$$\widehat{N}_{cr\omega}^{BS} = \left( \frac{1}{\widehat{N}_{cr\omega}^{B}} + \frac{1}{\frac{1}{i_{\omega}^{2}}\widehat{S}_{\omega\omega}} \right)^{-1}, \tag{45}$$

$\widehat{N}_{crz}^{B}$ and $\widehat{N}_{cr\omega}^{B}$ are given by Eqs. (2) and (4).

The polar radius of gyration of the cross-section about the shear center for an orthotropic beam is

$$i_{\omega}^{2} = z_{sc}^{2} + \frac{\widehat{EI}_{yy} + \widehat{EI}_{zz}}{\widehat{EA}}, \tag{46}$$

where $\widehat{EA}$ is the tensile stiffness of the composite beam.

We note that $\widehat{N}_{crz}^{BS}$ and $\widehat{N}_{cr\psi}^{BS}$ are the in-plane buckling and torsional buckling loads of a simply supported beam taking the shear deformations into account (Kollár, 2001a).

By this simplification of matrix $[Q]$ Eq. (39) yields

$$\begin{vmatrix} \widehat{N}_{crz}^{BS} & -M_{cr} \\ -M_{cr} & i_{\omega}^{2}\widehat{N}_{cr\psi}^{BS} + \beta_{1}M_{cr} \end{vmatrix} = 0. \tag{47}$$

By rearranging Eq. (47) we obtain

$$M_{cr}^{2} - \widehat{N}_{crz}^{BS}\beta_{1}M_{cr} - \widehat{N}_{crz}^{BS}\widehat{N}_{cr\psi}^{BS}i_{\omega}^{2} = 0. \tag{48}$$

Note that Eq. (48) is identical to Eq. (1), which was derived for a beam without shear deformation, if the following substitutions are made:

$$\widehat{N}_{crz}^{B} \to \widehat{N}_{crz}^{BS} = \left( \frac{1}{\widehat{N}_{crz}^{B}} + \frac{1}{\widehat{S}_{yy}} \right)^{-1}, \tag{49}$$

$$\widehat{N}_{cr\omega}^{B} \to \widehat{N}_{cr\omega}^{BS} = \left( \frac{1}{\widehat{N}_{cr\omega}^{B}} + \frac{1}{\frac{1}{i_{\omega}^{2}}\widehat{S}_{\omega\omega}} \right)^{-1}, \tag{50}$$

$$\widehat{N}_{cr\psi}^{B} \to \widehat{N}_{cr\psi}^{BS}, \tag{51}$$

where $\widehat{N}_{crz}^{B}$ and $\widehat{N}_{cr\omega}^{B}$ are given by Eqs. (2) and (4), and $\widehat{N}_{cr\psi}^{B}$ is given by Eq. (3) and $\widehat{N}_{cr\psi}^{BS}$ by Eq. (44).

The effect of neglecting $\widehat{S}_{y\omega}$ will be investigated in the numerical examples.

Eqs. (49)–(51) show that both the horizontal shear deformation (through $\widehat{S}_{yy}$) and the torsional shear deformation (through $\widehat{S}_{\omega\omega}$) reduce the critical moment ($M_{cr}$).

### 5.2. Uniformly distributed load

A simply supported beam subjected to a uniformly distributed load ($q$) is considered (Fig. 4(b)). The bending moment ($M_y$) is given by

$$M_{y} = q\frac{x(l-x)}{2}, \tag{52}$$

and the coefficients of the governing differential equations (Eqs. (18)–(20)) are not constant.

Following Chwalla's steps for beams without shear deformation (Kollár, 1999) we derive an approximate solution for the differential equations by using the Ritz method with one term approximation.

The potential energy of the beam is

$$\Pi = U + W, \tag{53}$$

where $U$ is the strain energy

$$U = \frac{\widehat{GI}_t}{2}\int_0^1 \vartheta^2\,\mathrm{d}x + \frac{\widehat{EI}_\omega}{2}\int_0^1 \Gamma^2\,\mathrm{d}x + \frac{\widehat{EI}_{zz}}{2}\int_0^1 \kappa_z^2\,\mathrm{d}x + \frac{\widehat{S}_{yy}}{2}\int_0^1 \gamma_y^2\,\mathrm{d}x + \frac{\widehat{S}_{\omega\omega}}{2}\int_0^1 \vartheta_{\mathrm{S}}^2\,\mathrm{d}x + 2\frac{\widehat{S}_{y\omega}}{2} \times \int_0^1 \gamma_y\vartheta_{\mathrm{S}}\,\mathrm{d}x, \tag{54}$$

and $W$ is the work done by the external load (Kollár, 1999)

$$W = -\frac{1}{2}\int_0^1 [-\beta_1 M_y\vartheta^2 - 2M_y\psi\kappa_z]\,\mathrm{d}x - \frac{-f}{2}\int_0^1 [q\psi^2]\,\mathrm{d}x. \tag{55}$$

We assume the following approximate displacement functions (which satisfy the boundary conditions Eqs. (31) and (32)):

$$\begin{aligned} v &= v_0\sin\frac{\pi x}{l}, \qquad \chi_y = \chi_0\cos\frac{\pi x}{l}, \\ \psi &= \psi_0\sin\frac{\pi x}{l}, \qquad \vartheta_{\mathrm{B}} = \vartheta_0^{\mathrm{B}}\cos\frac{\pi x}{l}. \end{aligned} \tag{56}$$

The deformation of the beam is illustrated in Fig. 1(b). The principle of stationary potential energy gives

$$\frac{\partial\Pi}{\partial\chi_0} = 0, \qquad \frac{\partial\Pi}{\partial\vartheta_0^{\mathrm{B}}} = 0, \tag{57}$$

$$\frac{\partial\Pi}{\partial\vartheta_0} = 0, \qquad \frac{\partial\Pi}{\partial\psi_0} = 0. \tag{58}$$

Substituting Eqs. (53)–(56) into Eq. (57) we obtain after algebraic manipulations

$$\left(\frac{\pi^2}{l^2}[\widehat{EI}] = [\widehat{S}]\right)\begin{Bmatrix}\chi_0\\ \vartheta_0^{\mathrm{B}}\end{Bmatrix} - \frac{\pi}{l}[\widehat{S}]\begin{Bmatrix}v_0\\ \psi_0\end{Bmatrix} = 0, \tag{59}$$

while substituting Eqs. (53)–(56) into Eq. (58) results in:

$$\left(\left(\frac{\pi^2}{l^2}[\widehat{S}] + \frac{\pi^2}{l^2}\begin{bmatrix}0 & 0\\ 0 & \widehat{GI}_t\end{bmatrix} + \frac{\pi^2}{l^2}q_{\mathrm{cr}}\begin{bmatrix}0 & -\frac{\pi^2+3}{12\pi^2}l^2\\ -\frac{\pi^2+3}{12\pi^2}l^2 & \frac{\pi^2-3}{12\pi^2}l^2\beta_1 + \frac{1}{\pi^2}l^2 f\end{bmatrix}\right)\begin{Bmatrix}v_0\\ \psi_0\end{Bmatrix} - \frac{\pi}{l}[\widehat{S}]\begin{Bmatrix}\chi_0\\ \vartheta_0^{\mathrm{B}}\end{Bmatrix}\right) = 0. \tag{60}$$

By eliminating $\chi_0$ and $\vartheta_0^{\mathrm{B}}$ from these two equations we obtain

$$\left([Q] + q_{\mathrm{cr}}\begin{bmatrix}0 & -\frac{\pi^2+3}{12\pi^2}l^2\\ -\frac{\pi^2+3}{12\pi^2}l^2 & \frac{\pi^2-3}{12\pi^2}l^2\beta_1 + \frac{1}{\pi^2}l^2 f\end{bmatrix}\right)\begin{Bmatrix}v_0\\ \psi_0\end{Bmatrix} = 0, \tag{61}$$

where $[Q]$ is given by Eq. (40).

The condition of the nontrivial solution is:

$$\left|[Q] + q_{\mathrm{cr}}\begin{bmatrix}0 & -\frac{\pi^2+3}{12\pi^2}l^2\\ -\frac{\pi^2+3}{12\pi^2}l^2 & \frac{\pi^2-3}{12\pi^2}l^2\beta_1 + \frac{1}{\pi^2}l^2 f\end{bmatrix}\right| = 0. \tag{62}$$

*Further approximation*: When the off diagonal terms in the shear stiffness matrix are zero or neglected ($\widehat{S}_{y\omega} = 0$), matrix $[Q]$ simplifies to Eq. (42) and Eq. (62) can be written in the form

$$\underbrace{\left(\frac{\pi^2+3}{12\pi^2}\right)^2}_{0.01181} l^4 q_{\mathrm{cr}}^2 - \left(\underbrace{\frac{\pi^2-3}{12\pi^2}}_{0.05800}\beta_1 + \underbrace{\frac{1}{\pi^2}}_{0.10132} f\right) l^2 \widehat{N}_{\mathrm{crz}}^{\mathrm{BS}} q_{\mathrm{cr}} - \widehat{N}_{\mathrm{crz}}^{\mathrm{BS}} \widehat{N}_{\mathrm{cr}\psi}^{\mathrm{BS}} i_\omega^2 = 0, \tag{63}$$

where $\widehat{N}_{\mathrm{crz}}^{\mathrm{BS}}$, $\widehat{N}_{\mathrm{cr}\psi}^{\mathrm{BS}}$ are defined by Eqs. (43) and (44). We note that Eq. (63) is identical to Eq. (7) if the substitutions given by Eqs. (49)–(51) are made.

### 5.3. Concentrated load at the midspan

We consider a simply supported beam subjected to a concentrated force ($P$) at the midspan (Fig. 4(c)). The Ritz method is applied to derive a closed form approximate solution for the buckling load. The function of the bending moment $M_y$ is

$$M_y = \begin{cases} \frac{P}{2}x, & \text{if } 0 \leqslant x \leqslant \frac{l}{2}, \\ \frac{P}{2}(l-x), & \text{if } \frac{l}{2} < x \leqslant l, \end{cases} \tag{64}$$

and the expression for the work done by the external load is (see Eq. (55))

$$W = -\frac{1}{2}\int_0^l \left[-\beta_1 M_y \vartheta^2 - 2M_y \psi \kappa_z\right] \mathrm{d}x - \frac{-f}{2} P (\psi_P)^2, \tag{65}$$

where $\psi_P$ is the rotation of the cross-section at the position of the applied load.

With the above bending moment and external work, following the same steps as in Section 5.2, we obtain the following equation for the critical load:

$$\left| [Q] + P_{\mathrm{cr}} \begin{bmatrix} 0 & -\frac{\pi^2+4}{8\pi^2} l \\ -\frac{\pi^2+4}{8\pi^2} l & \frac{\pi^2-4}{8\pi^2} l\beta_1 + \frac{2}{\pi^2} lf \end{bmatrix} \right| = 0. \tag{66}$$

By applying the $\widehat{S}_{y\omega} = 0$ approximation, we obtain

$$\underbrace{\left(\frac{\pi^2+4}{8\pi^2}\right)^2}_{0.03086} l^2 P_{\mathrm{cr}}^2 - \left(\underbrace{\frac{\pi^2-4}{8\pi^2}}_{0.07434}\beta_1 + \underbrace{\frac{2}{\pi^2}}_{0.20264} f\right) l \widehat{N}_{\mathrm{crz}}^{\mathrm{BS}} P_{\mathrm{cr}} - \widehat{N}_{\mathrm{crz}}^{\mathrm{BS}} \widehat{N}_{\mathrm{cr}\psi}^{\mathrm{BS}} i_\omega^2 = 0. \tag{67}$$

### 5.4. Two concentrated forces at the thirds of the span

When the beam is subjected to two concentrated forces (Fig. 4(d)) the buckling load can be determined similarly as in Section 5.3. The result, without giving the details, is

$$\left| [Q] + P_{\mathrm{cr}} \begin{bmatrix} 0 & -\frac{8\pi^2+27}{36\pi^2} l \\ -\frac{8\pi^2+27}{36\pi^2} l & \frac{8\pi^2-27}{36\pi^2} l\beta_1 + \frac{3}{\pi^2} lf \end{bmatrix} \right| = 0. \tag{68}$$

By applying the $\widehat{S}_{y\omega} = 0$ approximation, we have

$$\underbrace{\left(\frac{8\pi^2+27}{36\pi^2}\right)^2}_{0.08893} l^2 P_{\mathrm{cr}}^2 - \left(\underbrace{\frac{8\pi^2-27}{36\pi^2}}_{0.14623}\beta_1 + \underbrace{\frac{3}{\pi^2}}_{0.30396} f\right) l \widehat{N}_{\mathrm{crz}}^{\mathrm{BS}} P_{\mathrm{cr}} - \widehat{N}_{\mathrm{crz}}^{\mathrm{BS}} \widehat{N}_{\mathrm{cr}\psi}^{\mathrm{BS}} i_\omega^2 = 0. \tag{69}$$

### 5.5. General case

Eqs. (48), (63), (67), and (69) can be written in the form

$$M_{\mathrm{cr}} = C_1 \widehat{N}^{\mathrm{BS}}_{\mathrm{crz}} \left( C_2 f + C_3 \beta_1 + \sqrt{(C_2 f + C_3 \beta_1)^2 + \frac{\widehat{N}^{\mathrm{BS}}_{\mathrm{cr}\psi} i_\omega^2}{\widehat{N}^{\mathrm{BS}}_{\mathrm{crz}}}} \right), \tag{70}$$

where $C_1$, $C_2$ and $C_3$ are given in Table 1 and $\widehat{N}^{\mathrm{BS}}_{\mathrm{crz}}$ and $\widehat{N}^{\mathrm{BS}}_{\mathrm{cr}\psi}$, are given by Eqs. (43) and (44).

We observe that the buckling load for a simply supported beam can also be calculated such that the stiffnesses $\widehat{EI}_{zz}$ and $\widehat{EI}_{\omega}$ are modified due to the shear deformation in the formula of the buckling load of the corresponding beam without shear deformation (see Eq. (9)).

The necessary modifications are

| Beam without shear deformation | | Beam with shear deformation |
|---|---|---|
| $\widehat{EI}_{zz}$ | $\rightarrow$ | $\left( \frac{1}{\widehat{EI}_{zz}} + \frac{\pi^2}{(kl)^2} \frac{1}{\widehat{S}_{yy}} \right)^{-1}$, |
| $\widehat{EI}_{\omega}$ | $\rightarrow$ | $\left( \frac{1}{\widehat{EI}_{\omega}} + \frac{\pi^2}{(kl)^2} \frac{1}{\widehat{S}_{\omega\omega}} \right)^{-1}$, |

(71)

where $k = 1$ and $l$ is the total length of the simply supported beam.

By making the above substitutions in Eq. (9), it becomes identical to Eq. (70).

## 6. Cantilever beams

For cantilever beams the Ritz method with one term approximation significantly overestimates the buckling load even for the case of beams without shear deformation (Szatmári and Tomka, 1991). In order to obtain a satisfactory solution between ten and twenty terms are required in the analysis (see Roberts and Burt, 1985).

Using the analytical solution in Clark and Hill (1960), we arrive at Eq. (9) by substituting $kl$ for $l$, where $kl$ is the "effective" length. Clark and Hill (1960) gives $k = 1$ for a cantilever beam subjected to a uniformly distributed load or to a concentrated force at the end.

Here we suggest the modification of Eq. (9) (presented by Clark and Hill (1960) for beams without shear deformation), similarly as it was derived for simply supported beams.

Accordingly, the buckling load of a cantilever beam can be calculated from Eq. (9) when the stiffnesses are modified as shown in Eq. (71). In this equation $l$ is the total length of the cantilever and $k = 1$.

The accuracy of this solution will be investigated numerically in the next section.

## 7. Numerical examples

### 7.1. Simply supported beam with doubly symmetric cross-section

We consider a beam made of unidirectional carbon fiber reinforced epoxy. The Young modulus in the fiber direction is $E_1 = 148$ kN/mm$^2$ and the shear modulus is $G_{12} = 4.55$ kN/mm$^2$ (Tsai, 1988).

The cross-section of the beam is given in Fig. 7. The top and the bottom flanges are identical, $b_{f_1} = b_{f_2} = 120$ mm and $h_{f_1} = h_{f_2} = 5$ mm. The beam is simply supported at the ends, the length is $l = 1600$ mm.

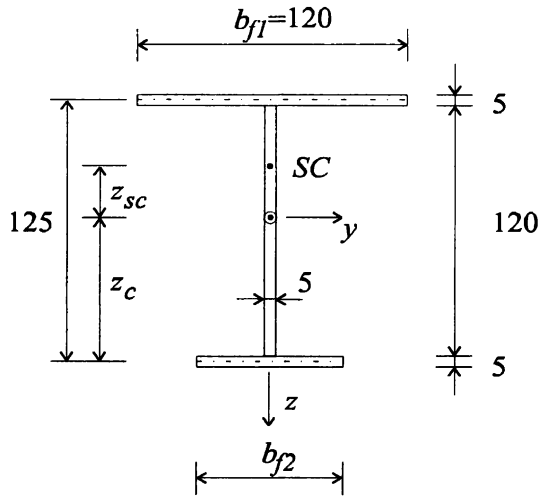


Fig. 7. Cross-section of a graphite epoxy composite I-beam.

The beam is subjected to concentrated moments at the ends. We determine the critical value of $M_{\mathrm{cr}}$ below. The beam is doubly symmetric, hence $z_{\mathrm{sc}} = \widehat{EI}_{yz} = \widehat{S}_{yz} = \widehat{S}_{z\omega} = 0$. The nonzero stiffnesses were calculated according to the expressions given in Appendix A. The cross-sectional properties presented in Table 2 (right column).

Eqs. (2), (4) and (3) give

$$\widehat{N}^{\mathrm{B}}_{\mathrm{cr}z} = 822\ \mathrm{kN}, \quad \widehat{N}^{\mathrm{B}}_{\mathrm{cr}\omega} = 843\ \mathrm{kN}, \quad \widehat{N}^{\mathrm{B}}_{\mathrm{cr}\psi} = 861\ \mathrm{kN}.$$

When shear deformation is neglected, the buckling load is calculated from Eq. (6). It gives

$$M^{\mathrm{B}}_{\mathrm{cr}} = 51.92\ \mathrm{kNm}.$$

Taking the shear deformation into account we have (Eqs. (43), (45) and (44))

$$\widehat{N}^{\mathrm{BS}}_{\mathrm{cr}z} = 696\ \mathrm{kN}, \quad \widehat{N}^{\mathrm{BS}}_{\mathrm{cr}\omega} = 714\ \mathrm{kN}, \quad \widehat{N}^{\mathrm{BS}}_{\mathrm{cr}\psi} = 732\ \mathrm{kN}.$$

With these values Eq. (6) gives

$$M^{\mathrm{BS}}_{\mathrm{cr}} = 44.06\ \mathrm{kNm}.$$

Table 2
The stiffnesses and geometrical parameters of the beams used for the numerical examples

| | $b_{f_2} = 60$ mm | $b_{f_2} = 120$ mm |
|---|---|---|
| $\widehat{EI}_{zz}$ (kN mm$^2$) | $120.07 \times 10^6$ | $213.3 \times 10^6$ |
| $\widehat{EI}_{\omega}$ (kN mm$^4$) | $185 \times 10^9$ | $832.5 \times 10^9$ |
| $\widehat{GI}_t$ (kN mm$^2$) | $0.057 \times 10^6$ | $0.068 \times 10^6$ |
| $\widehat{S}_{yy}$ (kN) | 3412.5 | 4550 |
| $\widehat{S}_{\omega\omega}$ (kN mm$^2$) | $14482 \times 10^3$ | $17773 \times 10^3$ |
| $\widehat{S}_{y\omega}$ (kN mm) | −94792 | 0 |
| $\beta_1$ (mm) | 84.83 | 0 |
| $i^2_{\omega}$ (mm$^2$) | 4514 | 3806 |
| $f_{\mathrm{top}}$ (mm) | −13.89 | −62.5 |
| $f_{\mathrm{bottom}}$ (mm) | 111.11 | 62.5 |

The same beam was investigated with the aid of a finite element program (ANSYS). Four node Mindlin shell elements were used with the maximum element size of 20 mm. The result is

$$M_{\mathrm{cr}}^{\mathrm{ANSYS}} = 44.19 \text{ kNm}.$$

Note that when only the transverse shear deformation is taken into account (but the shear deformation in warping is neglected) the buckling load is

$$M_{\mathrm{cr}} = 47.78 \text{ kNm}.$$

To show the effect of the shear deformation the buckling loads were calculated for different lengths of the beam. The results are given in Fig. 8.

The beam was also subjected to either a uniformly distributed load or to a concentrated force at the midspan. Trials were run applying the load at the shear center, the top flange, and the bottom flange.

The buckling load was calculated according to Eq. (70) with the appropriate $C_i$ parameters and using the finite element program. The result are given in Fig. 8.

### 7.2. Simply supported beam with monosymmetric cross-section

We consider a simply supported beam with the same material properties that are given in Section 7.1. The cross-section is given in Fig. 7. The top and the bottom flanges are different with $b_{f_1} = 120$ mm, $b_{f_2} = 60$ mm, hence the cross-section is monosymmetrical.

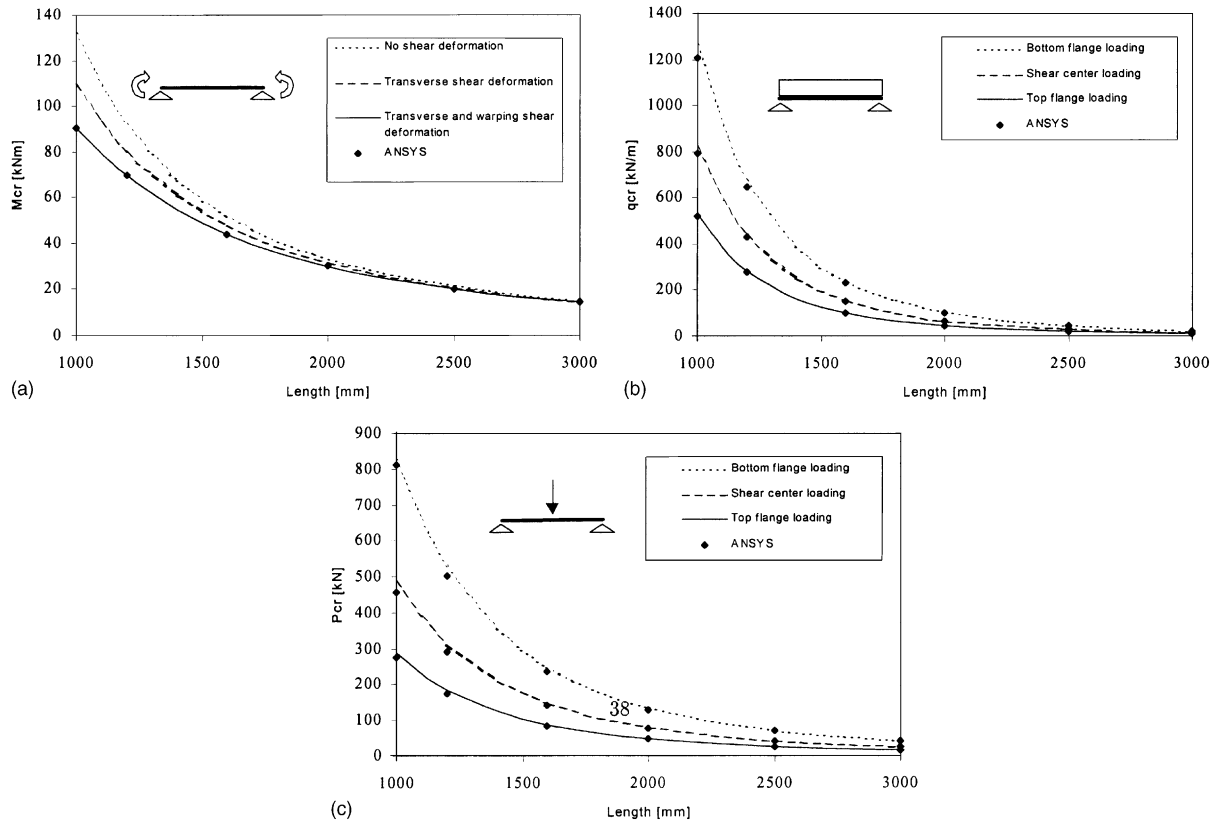


Fig. 8. Critical loads of the doubly symmetric simply supported beams.

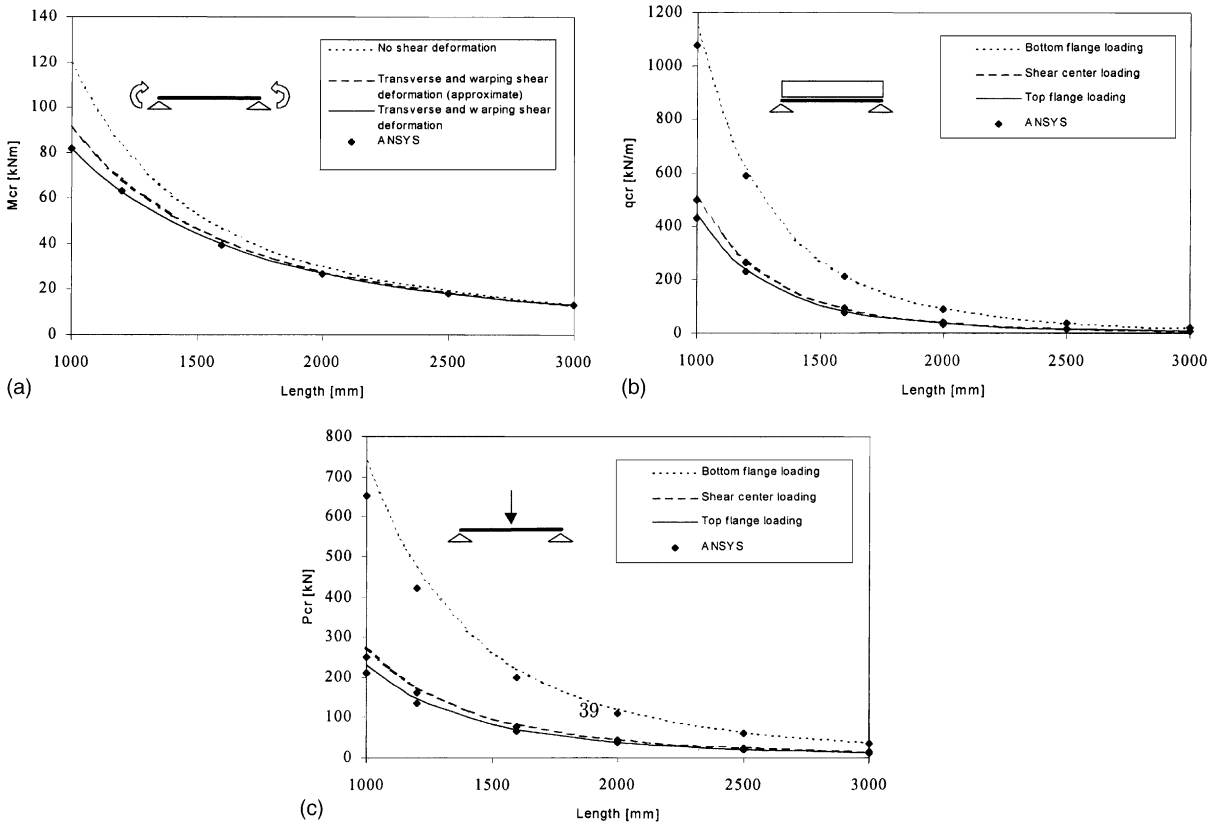


Fig. 9. Critical loads of the monosymmetric simply supported beams.

The beam is subjected to concentrated moments at the ends.

The properties of the cross-section were calculated according to the expressions given in Appendix A and according to Eqs. (21) and (25) and are given in the left column of Table 2.

The critical load was calculated from Eq. (39) for different lengths of the beam. The results are presented in Fig. 9 by solid line. These results show good agreement with the FE calculations which are also given in this figure.

The approximate buckling loads were also calculated by Eq. (6) taking the substitutions in Eq. (71) into account. These results are presented by a dashed line.

The figure shows that the shear deformation may significantly reduce the buckling load of short beams and that the suggested approximation is reasonable.

The beam was also subjected to either a uniformly distributed load or to a concentrated force at the midspan. The loads were applied either at the shear center, the top flange, or the bottom flange.

The buckling loads were calculated according to Eqs. (62) and (66) and by using the finite element program. The result are given in Fig. 9b and c.

### 7.3. Cantilever beam

A cantilever beam with the same material properties and cross-section given in Section 7.1 was considered. The beam was subjected to a uniformly distributed load and to a concentrated force at the end. The

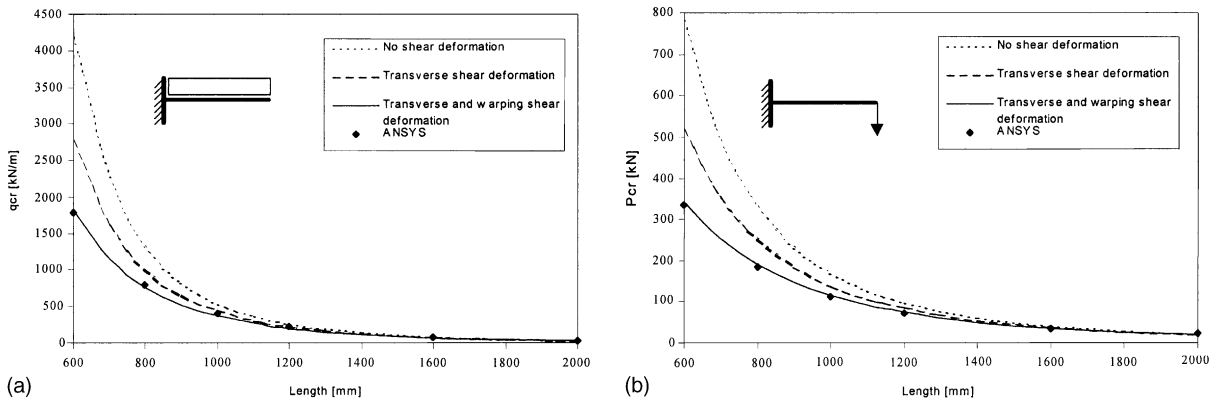


Fig. 10. Critical loads of the cantilever beams.

loading was applied at the shear center. Buckling loads were calculated according to Eq. (9) with the substitution suggested in Eq. (71) and by using the finite element program. The results are given in Fig. 10. It shows that for short beams the shear deformation reduces the buckling load, and the suggested calculation is reasonable.

### 7.4. Comparison with published results

Mottram (1992) investigated three E-glass reinforced pultruted doubly symmetric I-beams. Warping, twisting, and rotation about the minor axis ($z$) were restrained at the supports, only rotation about the major axis ($y$) was allowed. The beams were subjected to a concentrated force at the midspan applied at the top flange. In the general expression for the buckling load Eq. (9) the parameters are (Table 1): $k = 0.5$, $C_1 = 1.07$, $C_2 = 0.42$. The bending and warping stiffnesses were modified as proposed in Eq. (71) with $k = 0.5$. The calculated critical buckling load, taking the shear deformations into account, is $P_{cr}^{BS} = 5.1$ kN (and without shear deformation $P_{cr}^{B} = 5.5$ kN) which is in the upper range of the critical loads received from the experiments reported in range 2.8–5.75 kN. The higher loads belong to the cases where the behaviour of the beams were closer to the theoretical bifurcation. The lower critical load values show the great sensitivity due to geometric and loading imperfections and due to different uncertainties in the test set-up e.g. the support conditions did not give full restraints against warping and lateral rotation, which reduces the buckling load.

Zureick et al. (1995) analysed an E-glass doubly symmetric I-beam. The beam was simply supported and loaded at the third points with concentrated forces applied at the top flange. We determined the buckling load using Eq. (69): $P_{cr}^{BS} = 63.3$ kN (and without shear deformation $P_{cr}^{B} = 64.0$ kN) which is very close to the buckling load ($P_{cr} = 62.7$ kN) determined by FE analysis in Zureick et al. (1995).

Lin et al. (1996) analysed numerically (FE) simply supported doubly symmetric I-beams subjected to three different load conditions: concentrated moments at the ends, uniformly distributed load and a concentrated force at the midspan. The span of the beam was fixed and the critical loads were computed for various $E/G$ ratios. The same examples were solved using Eq. (70). The resulted critical loads coincide with the loads given by the FE analysis (the errors are within 1%). We calculated the critical loads by neglecting the effect of shear deformation and observed that the effect of shear deformation is negligible.

Sherbourne and Kabir (1995) published a method to determine the buckling load of doubly symmetric thin-walled fibrous composite beams. We tried to compare our results with Eqs. (27)–(29) and (32)–(34) of Sherbourne and Kabir (1995). However, these equations may contain a number of unknown typographical

mistakes and our effort therefore was unsuccessful. We wish to emphasize that our derived formulas offer the following advantages: our results are valid for cross-sections with one axis of symmetry, the beam can be loaded out of the shear center (e.g. top or bottom flange loading), the formulas derived in this article are simpler than those of Sherbourne and Kabir (1995).

## 8. Discussion

For composite beams the shear deformation may significantly reduce the lateral-torsional buckling load. This reduction can be taken into account if in the expression of the lateral-torsional buckling of beams (without shear deformation, Eq. (9)), the bending stiffness ($\widehat{EI}_{zz}$), and the warping stiffness ($\widehat{EI}_{\omega}$) are replaced as follows:

$$\widehat{EI}_{zz} \to \left( \frac{1}{\widehat{EI}_{zz}} + \frac{\pi^2}{(kl)^2} \frac{1}{\widehat{S}_{yy}} \right)^{-1}, \qquad \widehat{EI}_{\omega} \to \left( \frac{1}{\widehat{EI}_{\omega}} + \frac{\pi^2}{(kl)^2} \frac{1}{\widehat{S}_{\omega\omega}} \right)^{-1}. \tag{72}$$

Below we discuss the circumstances under which the shear deformation affects the buckling load significantly. To obtain simple result we consider a doubly symmetric beam loaded at the shear center, neglecting the torsional stiffness ($\widehat{GI}_t$), the critical bending moment is (Eq. (9))

$$M_{\mathrm{cr}} = C_1 \frac{\pi^2}{l^2} \sqrt{\widehat{EI}_{zz} \widehat{EI}_{\omega}}. \tag{73}$$

The effect of shear deformation is taken into account according to Eq. (71). The error, a result of neglecting the shear deformation is defined as

$$\alpha = \frac{M_{\mathrm{cr}}^{\mathrm{B}} - M_{\mathrm{cr}}^{\mathrm{BS}}}{M_{\mathrm{cr}}^{\mathrm{B}}}, \tag{74}$$

where $M_{\mathrm{cr}}^{\mathrm{B}}$ is the buckling load when the shear deformation is neglected, and $M_{\mathrm{cr}}^{\mathrm{BS}}$ is the buckling load when the shear deformation taken into account.

Introducing Eq. (72) and Eq. (73) the expression of the error yields to

$$\alpha = 1 - \frac{C_1 \frac{\pi^2}{l^2} \sqrt{\left( \frac{1}{\widehat{EI}_{zz}} + \frac{\pi^2}{l^2} \frac{1}{\widehat{S}_{yy}} \right)^{-1} \left( \frac{1}{\widehat{EI}_{\omega}} + \frac{\pi^2}{l^2} \frac{1}{\widehat{S}_{\omega\omega}} \right)^{-1}}}{C_1 \frac{\pi^2}{l^2} \sqrt{\widehat{EI}_{zz} \widehat{EI}_{\omega}}} = 1 - \frac{1}{\sqrt{\left( 1 + \frac{\pi^2}{l^2} \frac{\widehat{EI}_{zz}}{\widehat{S}_{yy}} \right) \left( 1 + \frac{\pi^2}{l^2} \frac{\widehat{EI}_{\omega}}{\widehat{S}_{\omega\omega}} \right)}}. \tag{75}$$

For a doubly symmetric I-beam (Appendix A)

$$\frac{\widehat{EI}_{zz}}{\widehat{S}_{yy}} \approx \frac{\widehat{EI}_{\omega}}{\widehat{S}_{\omega\omega}} \approx \frac{b^2}{10} \frac{E}{G},$$

and the above expressions (Eq. (75)) yields

$$\alpha = 1 - \frac{1}{1 + \frac{\pi^2}{10} \left( \frac{b}{l} \right)^2 \frac{E}{G}} \approx \left( \frac{b}{l} \right)^2 \frac{E}{G}, \tag{76}$$

where $b$ is the width of the flanges, $l$ is the span of the beam, $E$ is the Young modulus in the direction of the $x$-axis and $G$ is the shear modulus. (The second approximation is applicable if $\alpha$ is small, say $\alpha < 20\%$.)

For an isotropic beam $E/G \approx 2.5$, for a standard glass polyester pultruted profile $E/G$ is in the range of 5–10 while for a unidirectional carbon epoxy composite beam $E/G$ is in the range of 20–30. Consequently, the effect of shear deformation is significant for composite beams even if the ratio $l/b$ is high. This is illustrated below:

| $l/b$ | Isotropic | Glass reinforced (unidirectional fibers + mat) | | Unidirectional carbon epoxy | |
|---|---|---|---|---|---|
| $E/A$ | 2.5 | 5 | 10 | 20 | 30 |
| 5 | $\alpha = 9.0\%$ | $\alpha = 16.5\%$ | $\alpha = 28\%$ | $\alpha = 44\%$ | $\alpha = 54\%$ |
| 10 | $\alpha = 2.4\%$ | $\alpha = 4.7\%$ | $\alpha = 9.0\%$ | $\alpha = 16.5\%$ | $\alpha = 23\%$ |
| 15 | $\alpha = 1.1\%$ | $\alpha = 2.1\%$ | $\alpha = 4.2\%$ | $\alpha = 8.1\%$ | $\alpha = 11.6\%$ |
| 20 | $\alpha = 0.6\%$ | $\alpha = 1.2\%$ | $\alpha = 2.4\%$ | $\alpha = 4.7\%$ | $\alpha = 6.9\%$ |
| 40 | $\alpha = 0.15\%$ | $\alpha = 0.3\%$ | $\alpha = 0.6\%$ | $\alpha = 1.2\%$ | $\alpha = 1.8\%$ |

The error factor ($\alpha$) derived above for doubly symmetrical I-beams subjected at the shear center, can be applied, as an approximation for beams with different cross-sections and loading.

## 9. Conclusion

Explicit expressions were derived for the lateral-torsional buckling loads of composite beams. The effect of shear deformation can be taken into account by simply reducing the bending and warping stiffnesses of the composite beams (Eq. (71)). The derived results were verified by numerical examples.

## Acknowledgements

This work is supported by the Hungarian Science Foundation (OTKA, no T0 32053).

## Appendix A. Elastic properties of a monosymmetrical I-beam

In the following we present the elastic properties of a laminated (or pultruted) I-beam illustrated in Fig. 11.

The layup of the flanges and the web is symmetrical and orthotropic (and hence the matrix $[B]$ is zero, and the 1, 6 and 2, 6 elements of the $[A]$ and $[D]$ matrices are zero).

The tensile stiffness ($\widehat{EA}$) and the bending stiffnesses ($\widehat{EI}_{zz}$ and $\widehat{EI}_{yy}$) are (Barbero et al., 1993)

$$\widehat{EA} = \frac{b_{f_1}}{(a_{11})_{f_1}} + \frac{b_{f_2}}{(a_{11})_{f_2}} + \frac{b_{\mathrm{w}}}{(a_{11})_{\mathrm{w}}}, \tag{A.1}$$

$$\widehat{EI}_{zz} = \frac{b_{\mathrm{w}}}{(d_{11})_{\mathrm{w}}} + \frac{b_{f_1}^3}{12(a_{11})_{f_1}} + \frac{b_{f_2}^3}{12(a_{11})_{f_2}}, \tag{A.2}$$

$$\widehat{EI}_{yy} = \frac{b_{f_1}}{(a_{11})_{f_1}}(d - z_{\mathrm{c}})^2 + \frac{b_{f_2}}{(a_{11})_{f_2}} z_{\mathrm{c}}^2 + \frac{1}{(d_{11})_{f_1}} b_{f_1} + \frac{1}{(d_{11})_{f_2}} b_{f_2} + \frac{1}{(a_{11})_{\mathrm{w}}} \left( \frac{b_{w1}^3 + b_{w2}^3}{3} \right), \tag{A.3}$$

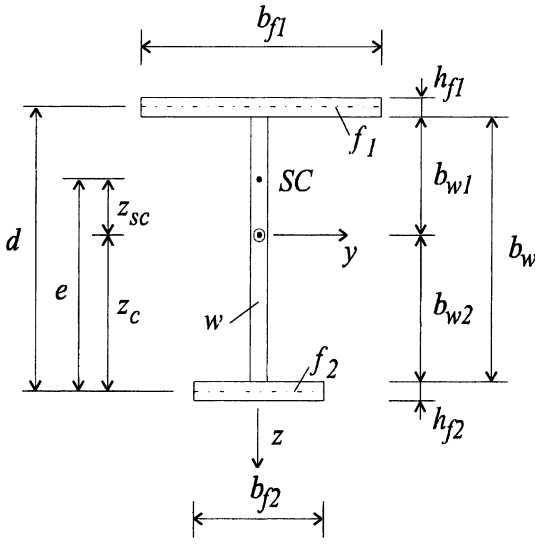


Fig. 11. Cross-section of a monosymmetric I-beam.

where subscripts $f_1$ and $f_2$ refer to the top and bottom flanges, and 'w' refers to the web. $a_{ij}$ and $d_{ij}$ are the elements of the compliance matrices of the laminate, and are calculated as

$$\begin{bmatrix} a_{11} & a_{12} & 0 \\ a_{12} & a_{22} & 0 \\ 0 & 0 & a_{66} \end{bmatrix} = \begin{bmatrix} A_{11} & A_{12} & 0 \\ A_{12} & A_{22} & 0 \\ 0 & 0 & A_{66} \end{bmatrix}^{-1}, \tag{A.4}$$

$$\begin{bmatrix} d_{11} & d_{12} & 0 \\ d_{12} & d_{22} & 0 \\ 0 & 0 & d_{66} \end{bmatrix} = \begin{bmatrix} D_{11} & D_{12} & 0 \\ D_{12} & D_{22} & 0 \\ 0 & 0 & D_{66} \end{bmatrix}^{-1}, \tag{A.5}$$

where $A_{ij}$ and $D_{ij}$ are the elements of the stiffness matrices of a laminate (Tsai, 1988) and must be calculated for the top flange ($f_1$), for the bottom flange ($f_2$), and for the web (w). In Eq. (A.3)

$$b_{w1} = b_w + \frac{h_{f_2}}{2} - z_c, \qquad b_{w2} = z_c - \frac{h_{f_2}}{2}, \tag{A.6}$$

where $z_c$ is the location of the centroid (i.e. the "center of gravity")

$$z_c = \frac{1}{\widehat{EA}} \left( \frac{b_{f_1}}{(a_{11})_{f_1}} d + \frac{b_w}{(a_{11})_w} \frac{d}{2} \right). \tag{A.7}$$

The torsional and warping stiffnesses are (Barbero et al., 1993)

$$\widehat{GI}_t = 4 \left( \frac{b_{f_1}}{(d_{66})_{f_1}} + \frac{b_{f_2}}{(d_{66})_{f_2}} + \frac{d}{(d_{66})_w} \right), \tag{A.8}$$

$$\widehat{EI}_\omega = \frac{b_{f_2}^3}{12(a_{11})_{f_2}} ed, \tag{A.9}$$

where the location of the shear center $e$ is

$$e = d\frac{b_{f_1}^3 \frac{1}{(a_{11})_{f_1}}}{b_{f_1}^3 \frac{1}{(a_{11})_{f_1}} + b_{f_2}^3 \frac{1}{(a_{11})_{f_2}}}. \tag{A.10}$$

The shear stiffness matrix $[\widehat{S}]$ is the inverse of the shear compliance matrix $[\hat{s}]$:

$$[\widehat{S}] = \begin{bmatrix} \widehat{S}_{yy} & 0 & \widehat{S}_{y\omega} \\ 0 & \widehat{S}_{zz} & 0 \\ \widehat{S}_{y\omega} & 0 & \widehat{S}_{\omega\omega} \end{bmatrix} = \begin{bmatrix} \hat{s}_{yy} & 0 & \hat{s}_{y\omega} \\ 0 & \hat{s}_{zz} & 0 \\ \hat{s}_{y\omega} & 0 & \hat{s}_{\omega\omega} \end{bmatrix}^{-1}, \tag{A.11}$$

where (Kollár, 2001b)

$$\hat{s}_{yy} = 1.2\left(\frac{(a_{66})_{f_1}}{b_{f_1}(1+\delta_{sc})^2} + \frac{(a_{66})_{f_2}}{b_{f_2}\left(1+\frac{1}{\delta_{sc}}\right)^2}\right), \tag{A.12}$$

$$\hat{s}_{zz} = \frac{(a_{66})_w}{d} + \frac{1}{12}\frac{(a_{66})_{f_1} b_{f_1}}{d^2} + \frac{1}{12}\frac{(a_{66})_{f_2} b_{f_2}}{d^2}, \tag{A.13}$$

$$\hat{s}_{\omega\omega} = \frac{1.2}{d^2}\left(\frac{(a_{66})_{f_1}}{b_{f_1}} + \frac{(a_{66})_{f_2}}{b_{f_2}}\right), \tag{A.14}$$

$$\hat{s}_{y\omega} = -\frac{1.2}{d}\left(-\frac{(a_{66})_{f_1}}{b_{f_1}(1+\delta_{sc})} + \frac{(a_{66})_{f_2}}{b_{f_2}\left(1+\frac{1}{\delta_{sc}}\right)}\right), \tag{A.15}$$

and

$$\delta_{sc} = \frac{d-(z_c+z_{sc})}{(z_c+z_{sc})} = \frac{d-e}{e}. \tag{A.16}$$

When the flanges and the web are made of a single orthotropic layer the expressions of $a_{11}$, $a_{66}$, $d_{11}$ and $d_{66}$ (Eqs. (A.4) and (A.5)) simplify to

$$a_{11} = \frac{1}{E_1 h}, \qquad a_{66} = \frac{1}{G_{12} h}, \qquad d_{11} = \frac{12}{E_1 h^3}, \qquad d_{66} = \frac{12}{G_{12} h^3},$$

where $E_1$ is the Young modulus in the direction of the beam's axis, $G_{12}$ is the in-plane shear modulus, and $h$ is the thickness of the laminate.

## References


Allen, H.G., Bulson, P.S., 1980. Background to Buckling. McGraw-Hill, London.

Anderson, J.M., Trahair, N.S., 1972. Stability of monosymmetric beams and cantilevers. Journal of the Structural Division, ASCE 98 (ST1), 269–286.

ANSYS, Finite Element Program Users Manual, Version 5.4, 1997. ANSYS Inc.

Barbero, E.J., Lopez-Anido, R., Davalos, J.F., 1993. On the mechanics of thin-walled laminated composite beams. Journal of Composite Materials 27, 806–829.

Brooks, R.J., Turvey, G.J., 1995. Lateral buckling of pultruted GRP I-Section cantilevers. Composite Structures 32 (1–4), 203–215.

Clark, J.W., Hill, H.N., 1960. Lateral buckling of beams. Journal of the Structural Division, ASCE 86 (ST7), 175–196.

Davalos, J.F., Qiao, P., 1997. Analytical and experimental study of lateral and distorsional buckling of FRP wide-flange beams. Journal of Composites for Construction 1 (4), 150–159.

Davalos, J.F., Qiao, P., Salim, H.A., 1997. Flexural-torsional buckling of pultruted fiber reinforced plastic composite I-beams: experimental and analytical evaluations. Composite Structures 38 (1-4), 241–250.

Engesser, F., 1889. Über die Knickfestigkeit gerader Stäbe. Zeitschrift für Architekten und Ingenieurwesen 35 (4), 455–462.

Galambos, T.V., 1998. Guide to Stability Design Criteria for Metal Structures, fifth ed. John Wiley & Sons, New York.

Helwig, T.A., Frank, K.H., Yura, J.A., 1997. Lateral-torsional buckling of singly symmetric I-beams. Journal of Structural Engineering 123 (9), 1172–1179.

Johnson, E.T., Shield, C.K., 1998. Lateral-torsional buckling of composite beams. In the proceedings of The Second International Conference on Composites in Infrastructure (ICCI'98), Tucson, Arizona, pp. 275–288.

Kollár, L., 1999. Special stability problems of beams and trusses. In: Kollár, L. (Ed.), Structural Stability in Engineering Practice. E & FN Spon, London.

Kollár, L.P., 2001a. Flexural-torsional buckling of open section composite columns with shear deformation. International Journal of Solids and Structures 38, 7525–7541.

Kollár, L.P., 2001b. Flexural-torsional vibration of open section composite beams with shear deformation. International Journal of Solids and Structures 38, 7543–7558.

Lin, Z.M., Polyzois, D., Shah, A., 1996. Stability of thin-walled pultruted structural members by the finite element method. Thin-Walled Structures 24 (1), 1–18.

Mottram, J.T., 1992. Lateral-torsional buckling of a pultruted I-beam. Composites 23 (2), 81–92.

Nethercot, D.A., 1973. The effective lengths of cantilevers as governed by lateral buckling. The Structural Engineer 51 (5), 161–168.

Nethercot, D.A., Rockey, K.C., 1971. A unified approach to the elastic lateral buckling of beams. The Structural Engineer 49 (7), 321–330.

Pandey, M.D., Kabir, M.Z., Sherbourne, A.N., 1995. Flexural-torsional stability of thin-walled composite I-section beams. Composites Engineering 5 (3), 321–342.

Roberts, T.M., Burt, C.A., 1985. Instability of monosymmetric I-beams and cantilevers. International Journal of Mechanical Sciences 27 (5), 313–324.

Roberts, T.M., Al-Ubaidi, H., 2001. Influence of shear deformation on restrained torsional warping of pultruted FRP bars of open cross-section. Thin-Walled Structures 39, 395–414.

Sherbourne, A.N., Kabir, M.Z., 1995. Shear strain effects in lateral stability of thin-walled fibrous composite beams. Journal of Engineering Mechanics 121 (5), 640–647.

Szatmári, I., Tomka, P., 1991. Analytical and numerical study on the lateral instability of a plated bridge. Periodica Polytechnica Ser. Civil Eng. 35 (3–4), 195–203.

Timoshenko, S.P., Gere, J.M., 1961. Theory of Elastic Stability, second ed. McGraw-Hill, New York.

Trahair, N.S., 1993. Flexural-Torsional Buckling of Structures. E & FN Spon, London.

Tsai, S.W., 1988. Composites Design. Think Composites, Dayton, fourth ed.

Turvey, G.J., 1996. Effects of load position on the lateral buckling response of pultruted GRP cantilevers—comparisons between theory and experiment. Composite Structures 35 (1), 33–47.

Wu, X., Sun, C.T., 1992. Simplified theory for composite thin-walled beams. American Institute of Aeronautics and Astronautics Journal 30 (12), 2945–2951.

Zureick, A., Kahn, L.F., Bandy, B.J., 1995. Tests on deep I-shape pultruted beams. Journal of Reinforced Plastics and Composites 14 (4), 378–389.